

# Velocity of Flowing Myoblast Cell at Oblique Micro Grooves

Shigehiro HASHIMOTO, Taku MATSUMOTO, Yuji ENDO, Shono KUWABARA, Hiroki YONEZAWA

Biomedical Engineering, Department of Mechanical Engineering, Kogakuin University

Tokyo, 163-8677, Japan

<http://www.mech.kogakuin.ac.jp/labs/bio/>

Kiyoshi YOSHINAKA

Health and Medical Research Institute, National Institute of Advanced Industrial Science & Technology

Tsukuba, 305-8564, Japan

## ABSTRACT

The velocity change of a flowing cell near the oblique micro groove on the bottom surface in the micro flow channel has been measured *in vitro*. The micro groove of the rectangular shape (4.5  $\mu\text{m}$  depth, and 0.2 mm length) has been fabricated on the polydimethylsiloxane (PDMS) disk by the photolithography technique. The angle between the flow direction and the longitudinal axis of the groove is 45 degree. Variation has been made on the width (0.03 mm, 0.04 mm, and 0.05 mm) of the groove. A rectangular flow channel (0.05 mm height  $\times$  1 mm width  $\times$  25 mm length) has been constructed between two transparent PDMS disks. In the test, malnourished C2C12 (mouse myoblast cell line) was used in comparison with the normal C2C12. A flow velocity ( $0.02 \text{ mm/s} < v_x < 0.23 \text{ mm/s}$ ) of the suspension of cells was controlled by the pressure difference between the inlet and the outlet. The change of the velocity (perpendicular to the main flow direction) of each flowing normal cell at the oblique groove is higher at the slower flowing velocity on the wider groove.

**Keywords:** Biomedical Engineering, C2C12, Malnourished Cell, Micro Groove and Velocity Change.

## 1. INTRODUCTION

The technology of sorting of cells can be applied to regenerative medicine to select the target cells [1]. It also can be applied to diagnostics to handle the target cell [2].

Several methods were proposed for the sorting of biological cells *in vitro*. The microfluidic systems were used in some methods. In these systems, variety of properties of cells were picked up for the sorting: electric, magnetic, dimension, or deformability [3, 4]. In the present study, physical properties have been picked up: diameter, and specific gravity.

To capture the target cell, several kinds of morphology were designed in the microfluidic systems: electrodes [5-8], micro slits [9, 10], micro holes [11, 12], or micro grooves [13-15]. The photolithography technique enables manufacturing the micro-morphology [16, 17]. The velocity of each cell can change at the groove on the bottom wall of the flow channel [15].

In the present study, the velocity of the single cell flowing over

the micro groove, which is manufactured by the photolithography technique, has been analyzed *in vitro*.

## 2. METHODS

### Micro Grooves

For changing the velocity of each cell, three micro grooves of the rectangular shapes (4.5  $\mu\text{m}$  depth, and 0.2 mm length) have been fabricated on the surface of the polydimethylsiloxane (PDMS) plate with the photolithography technique [15]. The grooves are arranged on the bottom of the micro flow channel. The angle between the flow direction and the longitudinal axis of the groove is 45 degree. At the groove arrangement from upstream to downstream, variation has been made on the width ( $w$ ) of the groove: 0.03 mm, 0.04 mm, and 0.05 mm.

### Flow System

Both the upper and the lower plates were exposed to the oxygen gas (0.1 Pa, 30  $\text{cm}^3/\text{min}$ ) in the reactive ion etching system (FA-1) (oxygen plasma ashing, 50 W, for thirty seconds). Immediately after ashing, the upper disk adheres (plasma bonding) to the lower disk to make the flow path (0.055 mm height  $\times$  1 mm width  $\times$  25 mm length) between them. The dimension of the width of each groove was measured on the microscopic image (Fig. 4). The flow channel is placed on the stage of the inverted phase-contrast microscope (IX71, Olympus Co., Ltd., Tokyo).

### Flow Test

C2C12 (passage  $< 10$ , mouse myoblast cell line originated with cross-striated muscle of C3H mouse) was used in the test. Cells were cultured with the D-MEM (Dulbecco's Modified Eagle's Medium) containing 10% FBS and 1% of Antibiotic-Antimycotic (penicillin, streptomycin and amphotericin B, Life Technologies) in the incubator for one week.

For comparison with normal cells (group A), malnourished cells (group B) were prepared. In the group B, cells were kept in the cryopreservation solution (the serum type Cellbanker1 (including dimethylsuloxide: Nippon Zenyaku Kogyo Co., Ltd, Koriyama, Japan)) in the incubator (at 310 K with 5% of  $\text{CO}_2$ ) for one week without medium change after cryopreservation.

The inner surface of the flow channel was hydrophilized by the oxygen (30  $\text{cm}^3/\text{min}$ , 0.1 Pa) plasma ashing for one minute at

100 W by the reactive ion etching system (FA-1), and prefilled with the bovine serum albumin solution for thirty minutes at 310 K.

Before the flow test, the cells were exfoliated from the plate of the culture dish with trypsin, and suspended in the D-MEM (Dulbecco's Modified Eagle's Medium). A part of the suspension of cells (4000 cells/cm<sup>3</sup>, 0.06 cm<sup>3</sup>) was poured at the inlet of the flow channel. The flow occurs by the pressure difference between the inlet and the outlet. The inlet hole (the depth of 3 mm and the diameter of 5 mm) makes the pressure head.

The residual part of the suspension of cells were continuously cultured in the medium for 30 minutes to confirm viability of cells by adhesion to the scaffold. The specific gravity of the cell was measured in comparison with the density of the phthalic acid ester solution between 1.05 g/cm<sup>3</sup> and 1.08 g/cm<sup>3</sup> by centrifuge.

Each cell rolling over the micro grooves was observed by the microscope, and recorded by the camera (DSC-RX100M4, Sony Corporation, Japan), which is set on the eyepiece of the microscope. Two-dimensional movement of each cell parallel to the bottom plane was analyzed by "Kinovea" at the video images (Fig. 1): 30 frames per second. At the images, the projected contour of each cell was traced with "Image J" (Fig. 2). The area ( $S$ ) enclosed by the outline was calculated. The equivalent diameter ( $D$ ) at the approximated circle was calculated by Eq. (1).

$$S = 0.25 \pi D^2 \quad (1)$$

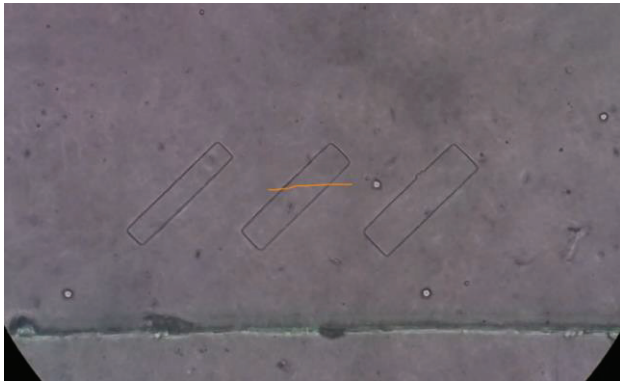


**Fig. 1:** Tracings (yellow line) of movement of cell passing over groove: left,  $w = 30 \mu\text{m}$ ; middle,  $w = 40 \mu\text{m}$ ; right,  $w = 50 \mu\text{m}$ : flow from left to right.



**Fig. 2:** Cell approaches to groove: contour of cell is traced: flow from left to right.

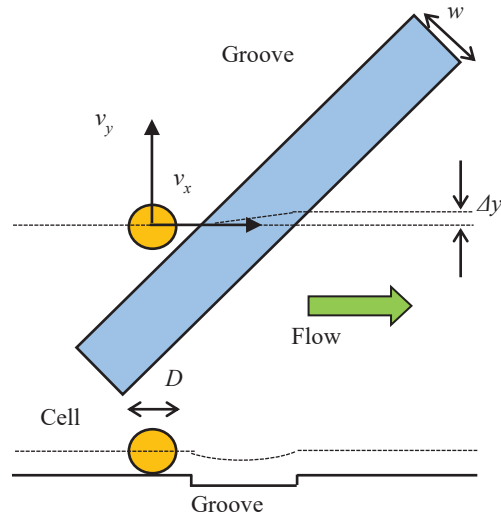


**Fig. 3:** Parameter of movement of cell passing over groove.

The velocity of each cell near the groove was traced on the components parallel ( $v_x$ ) and perpendicular ( $v_y$ ) to the direction of the main flow (Fig. 3). The shifted distance of each cell along the groove was traced on the component ( $\Delta y$ ) perpendicular to the main flow direction.

### 3. RESULTS

The density of the normal C2C12 (group A) was 1.065 g/cm<sup>3</sup>. The density of the malnourished C2C12 (group B) was lower than 1.06 g/cm<sup>3</sup>. Unlike cells of group A, cells of group B did not adhere to the scaffold within 30 minutes in the incubator. The diameter of each cell was in the range between 13.1  $\mu\text{m}$  and 21.7  $\mu\text{m}$ . The velocity of each cell ( $v_x$ ) immediately before the groove was in the range between 0.02 mm/s and 0.23 mm/s according to the pressure difference between the inlet and the outlet. The velocity gradually decreases with the time, because the pressure head at the inlet decreases with time. The tracings of the velocity of each cell are displayed in Fig. 4. Fig. 4a shows the component of the velocity parallel to the main flow direction ( $v_x$ ). Each cell flows at constant velocity

component on  $v_x$ . Fig. 4b shows the component of the velocity perpendicular to the main flow direction ( $v_y$ ). Each cell flows with the peak velocity component of  $v_y$  (three peaks: at  $x = -0.15$  mm, 0 mm, 0.15 mm) at each groove. The component of  $v_y$  is very small at the other part of the channel.

The shifted distances ( $\Delta y$ ) were in the range shorter than 10  $\mu\text{m}$  at each groove ( $w$ : 0.03 mm, 0.04 mm, and 0.05 mm). Data of the shifted distances ( $\Delta y$ ) are collected in relation to the area of each cell ( $S$ ) in Fig. 5: normal cells (Fig. 5a), and malnourished cells (Fig. 5b). The shifted distance ( $\Delta y$ ) at the groove ( $w = 0.04$  mm) scatters between 2  $\mu\text{m}$  and 10  $\mu\text{m}$ , when the area of each cell is in the range between 50  $\mu\text{m}^2$  to 350  $\mu\text{m}^2$ . The value of  $\Delta y$  tends to decrease with the area of each cell at the groove width of 0.04 mm, especially in the case of malnourished cells (Fig. 5b).

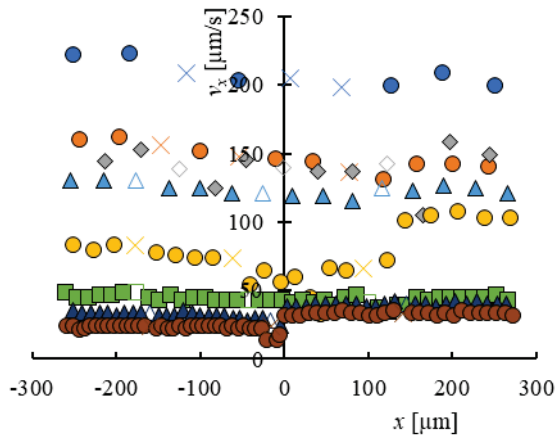


Fig. 4a: Position ( $x$ ) vs. velocity of cell ( $v_x$ ): the same color shows the same cell.

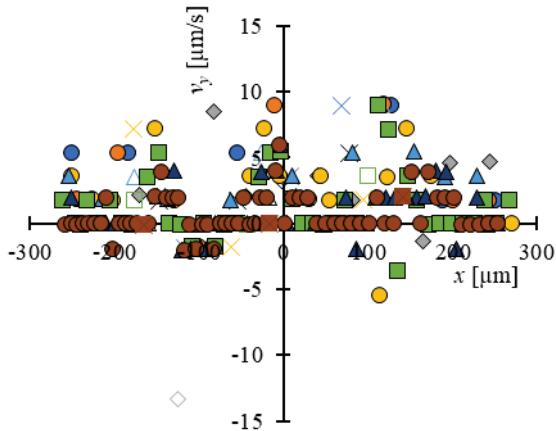


Fig. 4b: Position ( $x$ ) vs. velocity of cell ( $v_y$ ): the same color shows the same cell.

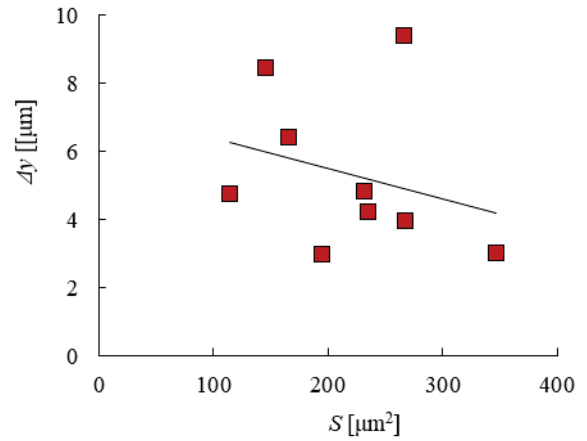


Fig. 5a:  $\Delta y$  vs. cell area ( $S$ ):  $w = 40$   $\mu\text{m}$ : normal cell: regression line ( $\Delta y = -0.0088 S + 7.3$ ): correlation coefficient,  $r^2 = 0.08$ .

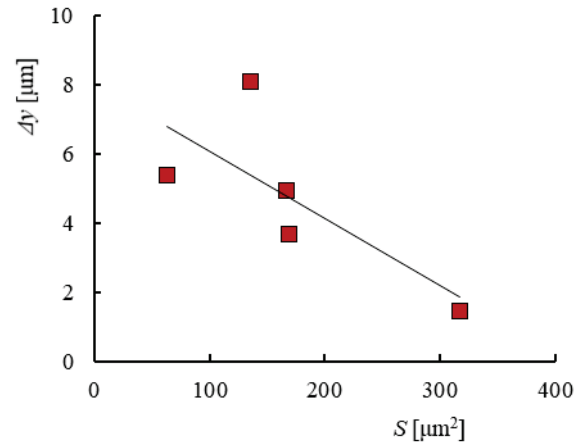
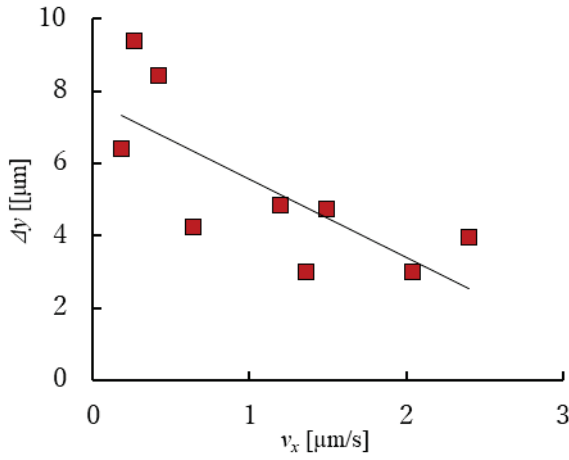


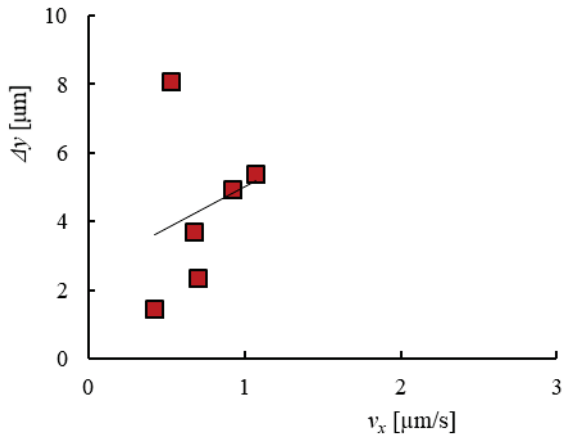
Fig. 5b:  $\Delta y$  vs. cell area ( $S$ ):  $w = 40$   $\mu\text{m}$ : malnourished cell: regression line ( $\Delta y = -0.020 S + 8.0$ ): correlation coefficient,  $r^2 = 0.55$ .

Fig. 6 shows relationships between the shifted distance ( $\Delta y$ ) and the velocity ( $v_x$ ) of each cell: normal cells (Fig. 6a), and malnourished cells (Fig. 6b). The value of  $\Delta y$  decreases with the velocity ( $v_x$ ) of each cell at the groove width of 0.04 mm in the case of normal cells (Fig. 6a).

Fig. 7 shows relationships between the velocity ratio ( $v_y \text{ max} / v_x$ ) and the length ratio ( $D / w$ ): normal cells (Fig. 7a), and malnourished cells (Fig. 7b). The velocity ratio is higher at normal cells than malnourished cells. At the normal cell, velocity component perpendicular to the main flow changes at the oblique groove more than at the malnourished cell. The velocity ratio is higher at the narrower width ( $w = 0.03$  mm) than at the wider width ( $w = 0.05$  mm). At some normal cells, the velocity ratio ( $v_y \text{ max} / v_x$ ) is higher at the small length ratio ( $D / w$ ).



**Fig. 6a:**  $\Delta y$  vs. velocity ( $v_x$ ):  $w = 40 \mu\text{m}$ : normal cell: regression line ( $\Delta y = -2.2 v_x + 7.7$ ): correlation coefficient,  $r^2 = 0.56$ .



**Fig. 6b:**  $\Delta y$  vs. velocity ( $v_x$ ):  $w = 40 \mu\text{m}$ : malnourished cell: regression line ( $\Delta y = 2.4 v_x + 2.6$ ): correlation coefficient,  $r^2 = 0.06$ .

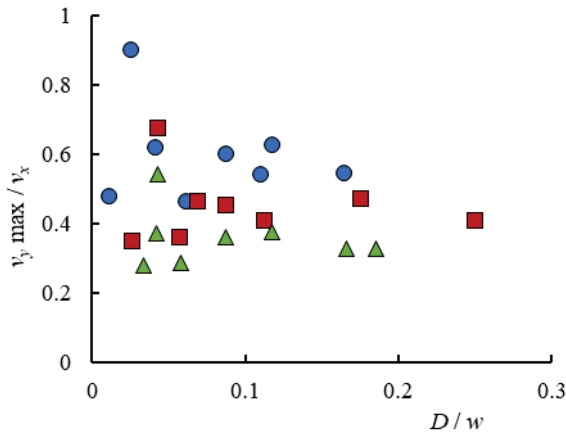


**Fig. 7a:** Velocity ratio ( $v_{y, \text{max}} / v_x$ ) vs.  $D/w$ : circle,  $w = 30 \mu\text{m}$ ; square,  $w = 40 \mu\text{m}$ ; triangle,  $w = 50 \mu\text{m}$ : normal cell.

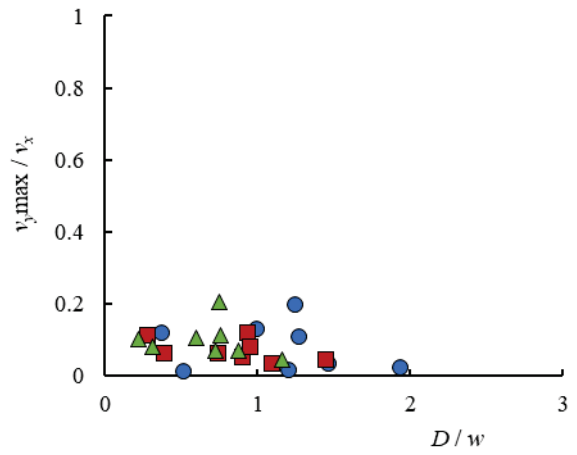


**Fig. 7b:** Velocity ratio ( $v_{y, \text{max}} / v_x$ ) vs.  $D/w$ : circle,  $w = 30 \mu\text{m}$ ; square,  $w = 40 \mu\text{m}$ ; triangle,  $w = 50 \mu\text{m}$ : malnourished cell.

#### 4. DISCUSSION

Filtration is one of the basic methods of sorting [18]. Fluorescence techniques [19-21] was used in the previous sorting systems with flow cytometry technique [22]. Non-destructive cell sorting systems, on the other hand, were designed in the previous studies [23]. The label-free methods were designed with microfluidic systems [24, 25]. Some of them were designed to capture cancer cells [26].

The microfluidic system was applied to sort biological cells [27-31], and to trap biological cells [32, 33]. The sorting technique might be applied to selection of cells for regenerative medicine and diagnostics of disease.

Several kinds of systems were designed for the cell sorting *in vitro* [9, 20, 21]. The micromachining technique has been applied to cell technology [34].

Several fluid flow systems were used in the previous studies. In the previous studies, cylindrical [11] and half cylindrical [12] holes were used for the trap of cells. The asymmetrical hole [12] might be suitable for trap than the symmetrical hole.

The rectangular grooves have been successfully manufactured on the wall of the micro fluid channel. The dimension of the grooves was confirmed by the laser microscope [13].

The depths of the micro patterns were between  $2 \mu\text{m}$  and  $10 \mu\text{m}$  in the previous studies [19-22]. In the present study, the depth of the grooves is  $4.5 \mu\text{m}$ , which is smaller than the diameter of the cells. The deeper hole may have advantage to trap every cell. At the shallower trap, on the other hand, it is not easy to tarp a cell. The trap of the appropriate dimension can distinguish cells. The duration of the trapped time of the cell might relate to interaction between the micro hole and the cell: affinity between the cell and the surface of the micro pattern, or deformability of the cell.

The results of the previous study show that the movement of cell travelling on the wall is modified by the oblique micro groove on the wall under the cell velocity lower than  $1 \text{ mm/s}$  [21]. The angle of 45 degrees between the longitudinal direction of the groove and the flow direction is effective to

shift the streamline of the cell. The shift movement along the oblique groove depends on the several parameters: the diameter of cells, the width of the groove, the velocity of the cell, and the cell types [13]. As the diameter of the cell decreases, the traveling length along the groove increases. The movement may be related not only to the diameter but also to deformability of the cell. Deformability was measured on red blood cells in previous studies [35].

The movement of flowing cell at the bottom surface of the flow channel may be related to the specific gravity of the cell: the density difference between the cell and the medium. The shifted distance of malnourished cells by the oblique groove was smaller than that of normal cells in the previous study [15].

In the present study, cells are sparsely suspended in the medium flow to reduce the interaction between cells. Cells can be sorted by the velocity change at the micro groove according to the diameter and the width of the groove [36].

## 5. CONCLUSION

The velocity change of a flowing C2C12 near the oblique micro groove on the bottom surface in the micro flow channel has been measured *in vitro*. The oblique micro groove of the rectangular shape (4.5  $\mu\text{m}$  depth, and 0.2 mm length) has been fabricated on the polydimethylsiloxane (PDMS) disk by the photolithography technique. The change of the velocity (perpendicular to the main flow direction) of each flowing normal cell at the oblique groove is higher at the slower flowing velocity on the wider groove of 0.05 mm.

## ACKNOWLEDGMENT

The authors thank to Mr. Akira Hayasaka for his assistance of the experiment.

## REFERENCES

- [1] M. Yamada, K. Kano, Y. Tsuda, J. Kobayashi, M. Yamato, M. Seki and T. Okano, "Microfluidic Devices for Size-dependent Separation of Liver Cells", **Biomed Microdevices**, Vol. 9, 2007, pp. 637–645.
- [2] Y.C. Ou, C.W. Hsu, L.J. Yang, H.C. Han, Y.W. Liu and C.Y. Chen, "Attachment of Tumor Cells to the Micropatterns of Glutaraldehyde (GA)-Crosslinked Gelatin", **Sensors and Materials**, Vol. 20, No. 8, 2008, pp. 435–446.
- [3] M. Kutschera and S. Kietaibl, "Deformability of Erythrocytes is Maintained after Autologous Cell Salvage in Orthopedic Surgery", **Journal of Anesthesia and Surgical Research**, Vol. 1, No. 1, 2020, pp. 1–9.
- [4] H. Lu and Z. Peng, "Boundary Integral Simulations of a Red Blood Cell Squeezing Through a Submicron Slit under Prescribed Inlet and Outlet Pressures", **Physics of Fluids**, Vol. 31, No. 031902, 2019, pp. 1–18. <https://doi.org/10.1063/1.5081057>
- [5] Y. Takahashi, S. Hashimoto, M. Watanabe and D. Hasegawa, "Dielectrophoretic Movement of Cell around Surface Electrodes in Flow Channel", **Journal of Systemics, Cybernetics and Informatics**, Vol. 16, No. 3, pp. 81–87, 2018.
- [6] S. Hashimoto, R. Matsuzawa and Y. Endo, "Analysis of Dielectrophoretic Movement of Floating Myoblast near Surface Electrodes in Flow Channel", **Proc. 11th International Multi-Conference on Complexity Informatics and Cybernetics**, Vol. 2, 2020, pp. 13–18.
- [7] N. A. Rahman, F. Ibrahim and B. Yafouz, "Dielectrophoresis for Biomedical Sciences Applications: A Review", **Sensors**, Vol. 17, No. 3, 2017, pp. 1–27.
- [8] X. Xing, M.L. Chau, K.A. Roshan and L. Yobas, "Dielectrophoretic Cell Sorting Via Sliding Cells on 3D Silicon Microelectrodes", **MEMS**, 2017, 2017, pp.147–150.
- [9] Y. Takahashi, S. Hashimoto, H. Hino and T. Azuma, "Design of Slit between Micro Cylindrical Pillars for Cell Sorting", **Journal of Systemics Cybernetics and Informatics**, Vol. 14, No. 6, 2016, pp. 8–14.
- [10] Y. Takahashi, S. Hashimoto, A. Mizoi and H. Hino, "Deformation of Cell Passing through Micro Slit between Micro Ridges Fabricated by Photolithography Technique", **Journal of Systemics Cybernetics and Informatics**, Vol. 15, No. 3, 2017, pp. 1–9.
- [11] S. Hashimoto, R. Nomoto, S. Shimegi, F. Sato, T. Yasuda and H. Fujie, "Micro Trap for Flowing Cell", **Proc. 17th World Multi-Conference on Systemics Cybernetics and Informatics**, Vol. 1, 2013, pp. 1–6.
- [12] S. Hashimoto, Y. Takahashi, H. Hino, R. Nomoto and T. Yasuda, "Micro Hole for Trapping Flowing Cell", **Proc. 18th World Multi-Conference on Systemics Cybernetics and Informatics**, Vol. 2, 2014, pp. 114–119.
- [13] Y. Takahashi, S. Hashimoto, H. Hino, A. Mizoi and N. Noguchi, "Micro Groove for Trapping of Flowing Cell", **Journal of Systemics, Cybernetics and Informatics**, Vol. 13, No. 3, 2015, pp. 1–8.
- [14] Y. Takahashi, S. Hashimoto, Y. Hori and T. Tamura, "Sorting of Cells Using Flow Channel with Oblique Micro Grooves", **Proc. 22nd World Multi-Conference on Systemics Cybernetics and Informatics**, Vol. 2, 2018, pp. 138–143.
- [15] S. Hashimoto, A. Hayasaka and Y. Endo, "Sorting of Cells with Flow Channel: Movement of Flowing Myoblast Cell at Oblique Micro Grooves", **Proc. 23rd World Multi-Conference on Systemics Cybernetics and Informatics**, Vol. 4, 2019, pp. 82–87.
- [16] A. Leclerc, D. Tremblay, S. Hadjiantoniou, N.V. Bukoreshtliev, J.L. Rogowski, M. Godin and A.E. Pelling, "Three-Dimensional Spatial Separation of Cells in Response to Microtopography", **Biomaterials**, Vol. 34, No. 33, 2013, pp. 8097–8104.
- [17] H. Hino, S. Hashimoto and F. Sato, "Effect of Micro Ridges on Orientation of Cultured Cell", **Journal of Systemics Cybernetics and Informatics**, Vol. 12, No. 3, 2014, pp. 47–53.
- [18] H.M. Ji, V. Samper, Y. Chen, C.K. Heng, T.M. Lim and L. Yobas, "Silicon-based Microfilters for Whole Blood Cell Separation", **Biomedical Microdevices**, Vol. 10, 2008, pp. 251–257.
- [19] A.Y. Fu, C. Spence, A. Scherer, F.H. Arnold and S.R. Quake, "A Microfabricated Fluorescence-Activated Cell Sorter", **Nature Biotechnology**, Vol. 17, 1999, pp. 1109–1111.
- [20] G. Mayer, M.S.L. Ahmed, A. Dolf, E. Endl, P.A. Knolle and M. Famulok, "Fluorescence-activated Cell Sorting for Aptamer SELEX with Cell Mixtures", **Nature Protocols**, Vol. 5, No. 12, 2010, pp. 1993–2004.
- [21] K. Mutaopoulos, P. Spink, C.D. Lofstrom, P.J. Lu, H. Lu, J.C. Sharpe, T. Franke and D.A. Weitz, "Traveling Surface Acoustic Wave (TSAW) Microfluidic Fluorescence

- Activated Cell Sorter ( $\mu$ FACS), **Lab on a Chip**, Vol. 2019, No. 19, 2019, pp. 2435–2443.
- [22] M. Brown and C. Wittwer, “Flow Cytometry: Principles and Clinical Applications in Hematology”, **Clinical Chemistry**, Vol. 46, No. 8B, 2000, pp. 1221–1229.
- [23] K. Takahashi, A. Hattori, I. Suzuki, T. Ichiki and K. Yasuda, “Non-destructive On-chip Cell Sorting System with Real-time Microscopic Image Processing”, **Journal of Nanobiotechnology**, Vol. 2, No. 5, 2004, pp. 1–8.
- [24] D.R. Gossett, W.M. Weaver, A.J. Mach, S.C. Hur, H.T.K. Tse, W. Lee, H. Amini and D. DiCarlo, “Label-free Cell Separation and Sorting in Microfluidic Systems”, **Analytical and Bioanalytical Chemistry**, Vol. 397, 2010, pp. 3249–3267.
- [25] T.R. Carey, K.L. Cotner, B. Li and L.L. Sohn, “Developments in Label-free Microfluidic Methods for Single-cell Analysis and Sorting”, **WIREs Nanomedicine and Nanobiotechnology**, Vol. 11, 2019, e1529, pp. 1–17.
- [26] Z. Liu, F. Huang, J. Du, W. Shu, H. Feng, X. Xu and Y. Chen, “Rapid Isolation of Cancer Cells Using Microfluidic Deterministic Lateral Displacement Structure”, **Biomicrofluidics**, Vol. 7, 011801, 2013, pp. 1–10.
- [27] M. Yamada, W. Seko, T. Yanai, K. Ninomiya and M. Seki, “Slanted, Asymmetric Microfluidic Lattices as Size-selective Sieves for Continuous Particle/cell Sorting”, **Lab on a Chip**, Vol. 17, 2017, pp. 304–314.
- [28] X. Wang, S. Chen, M. Kong, Z. Wang, K.D. Costa, R.A. Li and D. Sun, “Enhanced Cell Sorting and Manipulation with Combined Optical Tweezer and Microfluidic Chip Technologies”, **Lab on a Chip**, Vol. 11, No. 21, 2011, pp. 3656–3662.
- [29] Z. Zhang, W. Chien, E. Henry, D.A. Fedosov and G. Gompper, “Sharp-edged Geometric Obstacles in Microfluidics Promote Deformability-based Sorting of Cells”, **Physical Review Fluids**, Vol. 4, No. 2, 2019, pp. 1–18.
- [30] Y. Zheng, J. Nguyen, Y. Wei and Y. Sun, “Recent Advances in Microfluidic Techniques for Single-cell Biophysical Characterization”, **Lab on a Chip**, Vol. 13, 2013, pp. 2464–2483.
- [31] Y. Yoon, J. Lee, M. Ra, H. Gwon, S. Lee, M.Y. Kim, K.C. Yoo, O. Sul, C.G. Kim, W.Y. Kim, J.G. Park, S.J. Lee, Y.Y. Lee, H.S. Choi and S.B. Lee, “Continuous Separation of Circulating Tumor Cells from Whole Blood Using a Slanted Weir Microfluidic Device”, **Cancers**, Vol. 11, No. 200, 2019, pp. 1–13. doi:10.3390/cancers11020200
- [32] A. Khademhosseini, J. Yeh, S. Jon, G. Eng, K.Y. Suh, J.A. Burdick and R. Langer, “Molded Polyethylene Glycol Microstructures for Capturing Cells within Microfluidic Channels”, **Lab on a Chip**, Vol. 4, No. 5, 2004, pp. 425–430.
- [33] G. Simone, G. Perozziello, E. Battista, F. DeAngelis, P. Candeloro, F. Gentile, N. Malara, A. Manz, E. Carbone, P. Netti and E. DiFabrizio, “Cell Rolling and Adhesion on Surfaces in Shear Flow. A Model for an Antibody-Based Microfluidic Screening System”, **Microelectronic Engineering**, Vol. 98, 2012, pp. 668–671.
- [34] S. Lin, X. Zhi, D. Chen, F. Xia, Y. Shen, J. Niu, S. Huang, J. Song, J. Miao, D. Cui and X. Ding, “A Flyover Style Microfluidic Chip for Highly Purified Magnetic Cell Separation”, **Biosensors and Bioelectronics**, Vol. 129, 2019, 175–181.
- [35] J. Kim, H.Y. Lee and S. Shin, “Advances in the Measurement of Red Blood Cell Deformability: A brief Review”, **Journal of Cellular Biotechnology**, Vol. 1, 2015, pp. 63–79.
- [36] P.N. Carlsen, **Polydimethylsiloxane: Structure and Applications**, Nova Science Publishers, 2020, pp. 29–94.